Small, Water-Soluble, Ligand-Stabilized Gold Nanoparticles Synthesized by Interfacial Ligand Exchange Reactions

Marvin G. Warner, Scott M. Reed, and James E. Hutchison*

Department of Chemistry and Materials Science Institute, University of Oregon, Eugene, Oregon 97403-1253

Received May 10, 2000. Revised Manuscript Received August 3, 2000

A general synthetic approach leading to well-defined, water-soluble gold nanoparticles is described that involves a simple, interfacial ligand exchange reaction between a 1.4 nm phosphine-passivated precursor and an anionic or cationic thiol-containing ligand. We demonstrate the utility of this route by synthesizing water-soluble gold nanoparticles that are stabilized by either an anionic ligand (2-mercaptoethanesulfonate), a cationic ligand (2-(dimethylamino)ethanethiol hydrochloride), or a mixture of both ionic and phosphine ligands. Although the course of the ligand exchange process depends on the nature of the incoming ligand, each of these nanoparticle products retain the small core size and narrow size distribution of the starting particle (1.4 ± 0.4 nm). The stabilities of these nanoparticles to elevated temperature, extremes of pH, and added salt are reported and found to depend on the nature of the exposed headgroups on the ligand shell. Salt-induced aggregation is not observed in any of the cases investigated. Resistance to aggregation is attributed to the protective nature of the ligand shell.

Introduction

Ligand-stabilized metal nanoparticles have been extensively investigated due to interest in their unique physical properties,[1] chemical reactivity, and possible applications[2] (e.g., as bio-/chemosensors,[3] nanoelectronic components,[4] biological taggants,[5] and catalysts/catalyst supports[6]). To make use of these materials for fundamental or applied research, access to well-defined nanoparticle samples whose properties can be "tuned" through chemical modification is necessary. In a number of cases it has now been shown that, through careful choice of the passivating ligands and/or reaction conditions, one can produce nanoparticles tailored to possess desired properties.

Several synthetic approaches are commonly employed to produce small (1−5 nm) ligand-stabilized nanoparticles. A widely used preparation of organic-soluble nanoparticles is the method of Brust et al.,[7] in which $HAuCl_4$ is reduced in the presence of a thiol to yield nanoparticles with a variety of hydrophobic ligand shells.[1a] In some cases, the distribution of core sizes in these nanoparticles has been narrowed through fractional crystallization or electrophoretic methods.[8,9] We recently reported alternative syntheses in which alkanethiolate- or alkaneamine-passivated gold nanoparticles are prepared from narrow-dispersity phosphine-stabilized nanoparticles through ligand exchange reactions.[10,11] When the exchanging ligand is a thiol, the core size and dispersity are retained in the product.[10] Although these methods provide convenient access to gold nanoparticles soluble in nonpolar organic solvents, few synthetic methods for preparing water-soluble ligand-stabilized gold nanoparticles are available.

(1) (a) Brust, M.; Walker, M.; Bethell, D.; Schiffrin, D. J.; Whyman, R. *Chem. Commun.* **1994**, 801. (b) Whetten, R. L.; Khoury, J. T.; Alvarez, M. M.; Murthy, S.; Vezmar, I.; Wang, Z. L.; Stephens, P. W.; Cleveland, C. L.; Luedtke, W. D.; Landman, U. *Adv. Mater.* **1996**, *8*, 428. (c) Ingram, R. S.; Hostetler, M. J.; Murray, R. W. *J. Am. Chem. Soc.* **1997**, *119*, 9175. (d) Terrill, R. H.; Postlethwaite, T. A.; Chen, C.-h.; Poon, C.-D.; Terzis, A.; Chen, A.; Hutchison, J. E.; Clark, M. R.; Wignall, G.; Londono, J. D.; Superfine, R.; Falvo, M.; Johnson, C. S., Jr.; Samulski, E. T.; Murray, R. W. *J. Am. Chem. Soc.* **1995**, *117*, 12537.

(2) (a) Schön, G.; Simon, U. *Colloid Polym. Sci.* **1995**, *273*, 101. (b) Schön, G.; Simon, U. *Colloid Polym. Sci.* **1995**, *273*, 202. (c) Andres, R. P.; Bein, T.; Dorogi, M.; Feng, S.; Henderson, J. I.; Kubiak, C. P.; Mahoney, W.; Osifchin, R. G.; Reifenberger, R. *Science* **1996**, *272*, 1323. (d) Janes, D. B.; Kolagunta, V. R.; Osifchin, R. G.; Bielefeld, J. D.; Andres, R. P.; Henderson, J. I.; Kubiak, C. P. *Superlattices Microstruct.* **1995**, *18*, 275. (e) Feldheim, D. L.; Grabar, K. C.; Natan, M. J.; Mallouk, T. E. *J. Am. Chem. Soc.* **1996**, *118*, 7640. (f) Averin, D. V.; Likharev, K. K. *J. Low Temp. Phys.* **1986**, *62*, 345.

(3) (a) Mirkin, C. A.; Letsinger, R. L.; Mucic, R. C.; Storhoff, J. J. *Nature* **1996**, *382*, 607. (b) Storhoff, J. J.; Mirkin, C. A. *Chem. Rev.* **1999**, *99*, 1849. (c) Elghanian, R.; Storhoff, J. J.; Mucic, R. C.; Letsinger, R. L.; Mirkin, C. A. *Science* **1997**, *277*, 1078. (d) Storhoff, J. J.; Elghanian, R.; Mucic, R. C.; Mirkin, C. A.; Letsinger, R. L. *J. Am. Chem. Soc.* **1998**, *120*, 1959.

(4) Montemerlo, M. S.; Love, J. C.; Opiteck, G. J.; Goldhaber-Gordon, D.; Ellenbogen, J. C. *Technologies and Designs for Electronic Nanocomputers*; MITRE Technical Report No. 96W0000044; MITRE Corp.: McLean, VA, 1996.

(5) *Colloidal Gold: Principles, Methods, and Applications*; Hayat, M. A., Ed.; Academic Press: San Diego, CA, 1991.

(6) (a) Zhang, Z.; Cui, Z. *J. Mater. Sci. Technol.* **1998**, *14*, 395. (b) Oku, T.; Suganuma, K. *Chem. Commun.* **1999**, *23*, 2355. (c) Seery, T. A.; Dhar, P.; Huber, D. L.; Vatansever, F. *Polym. Prepr. (Am. Chem. Soc., Div. Polym. Chem.)* **1999**, *40*, 148. (d) Takei, H. *J. Vac. Sci. Technol. B* **1999**, *17*, 1906.

(7) Brust, M.; Fink, J.; Bethell, D.; Schriffin, D. J.; Kiely, C. *Chem. Commun.* **1995**, 1655.

(8) Schaaff, T. G.; Knight, G.; Shafigullin, M. N.; Borkman, R. F.; Whetten, R. L. *J. Phys. Chem. B* **1998**, *102*, 10643.

(9) Schaaff, T. G.; Whetten, R. L. *J. Phys. Chem. B* **2000**, *104*, 2630.

(10) Brown, L. O.; Hutchison, J. E. *J. Am. Chem. Soc.* **1997**, *119*, 12384.

(11) Brown, L. O.; Hutchison, J. E. *J. Am. Chem. Soc.* **1999**, *121*, 882.

10.1021/cm0003875 CCC: $19.00
Published on Web 10/03/2000

Two approaches have been investigated for the generation of water-soluble nanoparticles, direct synthesis and ligand place exchange reactions. Small, water-soluble nanoparticles have been prepared directly by sodium citrate reduction of $HAuCl_4$(aq) in the presence of 3-mercaptopropionic acid. The resulting nanoparticles range in size from 2.3 to 8.6 nm.[12] Sodium borohydride reductions of aqueous solutions of $HAuCl_4$ in the presence of several different water-soluble ligands including a tripeptide (glutathione),[8,9] *p*-thiophenol,[13] or tiopronin (*N*-2-mercaptopropionylglycine)[14,15] have also been reported. These reductions produce nanoparticles of varying sizes: from <1 to >5 nm, ≈5 nm, and from 1.8 to 3.9 nm, respectively. Ligand place exchange reactions have also been used to prepare water-soluble nanoparticles. The exchange of a water-soluble phosphine ligand, $Ph_2PC_6H_5SO_3Na$, onto $Au_{55}(PPh_3)_{12}Cl_6$ affords small, narrow-dispersity, water-soluble nanoparticles.[16] In another example of this approach different ligands can be exchanged for the extant ligands of water-soluble tiopronin-stabilized nanoparticles[14] to yield nanoparticles with a mixed ligand shell composition.[15]

A general synthetic method capable of producing a wide variety of water-soluble nanoparticles possessing a high degree of stability, peripheral chemical functionality, and small size has not been reported. Such nanoparticles are needed for applications in aqueous media (e.g., as biochemical supports and probes). We report here a versatile synthetic approach for preparing water-soluble, ligand-stabilized nanoparticles through interfacial ligand exchange reactions between a 1.4 nm phosphine-stabilized nanoparticle dissolved in a nonaqueous solvent and cationic or anionic thiol ligands in water. This simple and versatile approach yields water-soluble nanoparticles that maintain the small core size ($d_{CORE} \approx 1.4$ nm) and narrow dispersity of their precursor. In all cases the thermal stability of the products exceeds that of the phosphine-stabilized nanoparticles. These nanoparticles do not aggregate in the presence of high concentrations of salt. Decomposition without aggregation can occur in the presence of added salt depending upon the nature of the terminal functional group on the thiol ligand.

Experimental Section

Materials. Hydrogen tetrachloroaurate was purchased from Strem and was used as received. All other compounds were purchased from Aldrich and used as received. Methylene chloride was distilled over calcium hydride prior to use. Triphenylphosphine-stabilized nanoparticles **1** were synthesized by a previously described route[17] or a newly developed route.[18] In either instance the starting nanoparticle **1** has an average size of 1.4 nm.

General Preparation of Water-Soluble Gold Nanoparticles. A solution of **1** in dichloromethane was added to an aqueous solution of the water-soluble ligand. The biphasic reaction mixture was stirred rapidly to ensure good contact between the layers to facilitate the exchange reaction. Transfer of the darkly colored nanoparticles from the organic to the aqueous phase occurs over the course of the reaction. The rate of transfer depends on the incoming ligand. Upon completion of the exchange the aqueous layer was removed and washed with a series of solvents to remove excess ligand. Water was evaporated under a stream of nitrogen at room temperature. Crude material was washed with a second series of solvents to further ensure the removal of unbound, excess ligand. Removal of excess ligand is monitored using thin-layer chromatography and ^{1}H NMR. Solubilities of each of the product nanoparticles are reported for a number of common solvents.

Synthesis of 2-(Dimethylamino)ethanethiol Hydrochloride-Stabilized Nanoparticles (2). A sample of nanoparticle **1** in dichloromethane (30 mg in 4 mL) and 2-(dimethylamino)ethanethiol hydrochloride in water (9 mg in 4 mL) were used in the general procedure described above. Complete transfer of the darkly colored nanoparticles from the organic phase to the aqueous phase took place within 15 min. The aqueous layer was washed with dichloromethane (2 × 60 mL) prior to evaporation of the water. This crude product was precipitated once from ethanol with hexanes and transferred to a frit where it was washed with chloroform (2 × 60 mL) to remove excess ligand. The final product is soluble in water or mixtures of water with polar organic solvents such as alcohols; it is insoluble in nonpolar organic solvents such as dichloromethane, hexanes, and anhydrous tetrahydrofuran.

Synthesis of Mercaptoethanesulfonate/Triphenylphosphine-Stabilized Nanoparticles (3). A sample of nanoparticle **1** in dichloromethane (2 mg in 2 mL) and sodium 2-mercaptoethanesulfonate in water (4 mg in 2 mL) were used in the general procedure described above. Transfer of the darkly colored nanoparticles from the organic phase to the aqueous phase took place within 4 h. The aqueous layer was washed with dichloromethane (2 × 20 mL). After removal of the water, this material was suspended in methanol and transferred to a frit where it was washed with methanol (30 mL) and methylene chloride (30 mL) to remove excess ligand. The product is soluble in water or mixtures of water with polar organic solvents such as alcohols or tetrahydrofuran; it is insoluble in nonpolar organic solvents such as methylene chloride, hexanes, anhydrous methanol, and anhydrous tetrahydrofuran.

Synthesis of Mercaptoethanesulfonate-Stabilized Nanoparticles (4). A solution of **3** (2 mg in 3 mL of 1:1 tetrahydrofuran/water) and sodium 2-mercaptoethansulfonate (3 mg) was prepared. The mixture reaction was stirred for 12 h. After removal of the solvent, the material was suspended in methanol and transferred to a frit where it was washed with methanol (30 mL) and methylene chloride (30 mL) to remove excess ligand. This product is soluble in water or mixtures of water with polar organic solvents such as alcohols or tetrahydrofuran; it is insoluble in anhydrous organic solvents.

Synthesis of Mercaptoethanesulfonate/TFET-Stabilized Nanoparticles (5). A sample of **3** (2 mg in 3 mL of 8:1 methanol/ water) and trifluoroethanethiol (TFET) (20 mg) were added to the reaction vessel and the mixture was stirred for 45 min at ambient temperature. The sample was purified by washing the reaction mixture with hexanes (3 × 2 mL), methylene chloride (3 × 2 mL), and hexanes (3 × 2 mL).

Measurements. X-ray photoelectron spectroscopy (XPS) was performed on a Kratos HSi instrument operating at a base pressure of ~ 10^{-8} mmHg using monochromatic Al Kα radiation at 15 mA and 15 kV. Nanoparticle samples were drop cast

(12) Yonezawa, T.; Sutoh, M.; Kunitake, T. *Chem. Lett.* **1997**, 619.
(13) Chen, S. *Langmuir* **1999**, *15*, 7551.
(14) Templeton, A. C.; Chen, S.; Gross, S. M.; Murray, R. W. *Langmuir* **1999**, *15*, 66.
(15) Templeton, A. C.; Cliffel, D. E.; Murray, R. W. *J. Am. Chem. Soc.* **1999**, *121*, 7081.
(16) Schmid, G.; Klein, N.; Korste, L.; Kriebig, U.; Schonauer, D. *Polyhedron* **1988**, *7*, 605.
(17) (a) Schmid, G. *Inorg. Synth.* **1990**, *27*, 214. (b) Schmid, G.; Pfeil, R.; Boese, R.; Bandermann, F.; Meyer, S.; Calis, G. H. M.; van der Velden, J. W. A. *Chem. Ber.* **1981**, *114*, 3634. (c) Rapoport, D. H.; Vogel, W.; Cölfen, H.; Schlögl, R. *J. Phys. Chem. B* **1997**, *101*, 4175.

(18) Nanoparticles were synthesized according to a new route. All results presented were performed on phosphine nanoparticles prepared according to ref 17a; however, synthesis of **2**, **3**, and **4** has been successfully repeated using nanoparticles from this new route. Weare, W. W.; Reed, S. R.; Warner, M. G.; Hutchison, J. E. *J. Am. Chem. Soc.*, submitted for publication.

from a dilute aqueous solution onto a clean glass slide. Samples were charge compensated and binding energies were referenced to carbon 1s at 284.4 eV. UV−visible spectroscopy was performed on a Hewlett-Packard HP 8453 diode array instrument with a fixed slit width of 1 nm using 1-cm quartz cuvettes. ^{1}H NMR spectra were recorded with a Varian-Inova spectrometer at a frequency of 300 MHz.

Transmission electron microscopy (TEM) was performed on a Philips CM-12 microscope operating at a 120-kV accelerating voltage. Samples were deposited by aerosol onto carbon-coated 400-mesh nickel grids (Ted Pella). Excess water was blotted off the grids with filter paper and then the samples were dried under ambient conditions prior to inspection by TEM. Images were recorded and processed as described previously.[19]

Results and Discussion

The simple interfacial ligand place exchange method described allows preparation of ionically substituted water-soluble nanoparticles, starting from organic-soluble phosphine-stabilized nanoparticles.[17,18] This general route is amenable to both cationic and anionic ligands; however, the observed reaction pathway depends on the chemical functionality of the incoming ligand. In each case the metal core diameter is preserved during the exchange. Furthermore, the product nanoparticles exhibit greater thermal stability than the phosphine-passivated starting material and do not aggregate in the presence of added salt.

Interfacial Ligand Exchange Reactions. The extent of ligand exchange in each case depends on the nature of the incoming ligand. Replacement of the triphenylphosphine ligands by a cationic thiol ligand, (2-dimethylamino)ethanethiol hydrochloride[20] (Scheme 1, step d), proceeds to completion rapidly to produce nanoparticle **2**. The absence of phosphorus in the XPS spectra and aromatic signals in the ^{1}H NMR spectra suggest that all phosphine ligands have been removed from the nanoparticle in the purified material. The ^{1}H NMR spectrum of **2** shows no sign of free ligand or AuCl(PPh_3) (a byproduct[19] of the exchange reaction). The absence of a plasmon resonance[21] at 520 nm in the UV−vis spectrum suggests that the small size of the starting nanoparticle **1** is preserved in **2** after the exchange reaction.

Replacement of triphenylphosphine ligands with the anionic thiol ligand, 2-mercaptoethanesulfonate, occurs in a two-step process (Scheme 1, steps a and b). In the first step, facile exchange of the phosphine ligands by thiol ligands results in intermediate **3**. The ligand shell of **3** contains a mixture of thiol and phosphine ligands as evidenced by both XPS and ^{1}H NMR data. The ratio of phosphorus to sulfur measured by XPS is ≈2:5. The ^{1}H NMR spectrum of **3** contains broad peaks in both the aliphatic and aromatic regions, consistent with the presence of triphenylphosphine and 2-mercaptoethanesulfonate bound to the surface of the nanoparticle. The absence of sharp resonances in either region confirms the absence of free ligand. The lack of the plasmon resonance in the UV−vis spectrum suggests the preservation of the small gold core size.

Scheme 1[a]

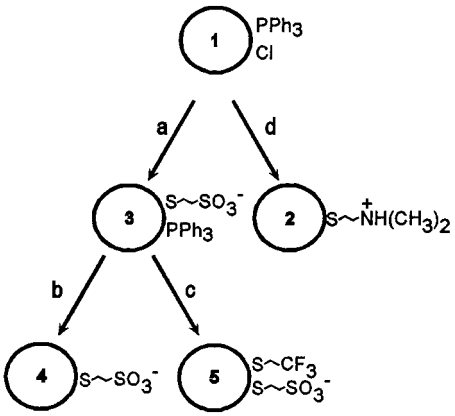

[a] Conditions (a) interfacial ligand exchange of **1** in CH_2Cl_2 with sodium 2-mercaptoethanesulfonate in water produces nanoparticle **3**, which contains a mixed ligand shell; (b) nanoparticle **3** treated with excess ligand in a 1:1 THF/water mixture yields nanoparticle **4** or (c) can be reacted with 2,2,2-trifluoroethanethiol to yield nanoparticle **5** with a mixed ligand shell; (d) interfacial ligand exchange of **1** in CH_2Cl_2 with (*N*,*N*-dimethylamino)ethanethiol hydrochloride in water occurs in a one-step process to yield nanoparticle **2**.

Intermediate **3** is a useful precursor to fully 2-mercaptoethanesulfonate-substituted particle **4** or to water-soluble particles containing additional functional ligands (e.g., 2,2,2-trifluoroethanethiol). Completion of the ligand exchange reaction to yield nanoparticle **4** is performed in a 1:1 THF/water mixture. In **4** all phosphine ligands have been replaced by 2-mercaptoethanesulfonate as evidenced by both XPS and ^{1}H NMR. We investigated the exchange of 2,2,2-trifluoroethanthiol (TFET) (Scheme 1, step c) into the ligand shell of nanoparticle **3** to generate nanoparticle **5**. TFET was chosen because it is easily observed in XPS analysis. Nanoparticle **5** was examined by XPS after purification and showed the presence of sulfur, fluorine, and phosphorus providing evidence for a mixed ligand shell nanoparticle.

We hypothesize that the retention of phosphine ligands on intermediate **3** is due to the difficulty of dissociating a phosphine ligand from the nanoparticle once it has transferred to the aqueous phase. Transfer of the nanoparticle and arrest of the exchange reaction occur after a fraction of water-soluble 2-mercaptoethanesulfonate ligands have replaced the triphenylphosphine ligands. This is evidenced by little change in the composition of **3**, even at very high ligand-to-nanoparticle ratios (as high as 200:1 has been tried). The facile formation of nanoparticle **4** in a 1:1 THF/water mixture demonstrates that conditions which increase the solubility of the dissociated phosphine ligands allow complete exchange to occur.

In the production of the cationic nanoparticle **2**, the exchange does not produce an isolable dual-ligand intermediate, suggesting that complete exchange occurs either in the organic phase or at the interface. This observation may be explained by the greater solubility of the free cationic ligand in organic solvent (relative to the solubility of the free sulfonate ligand), resulting in

(19) Studies performed previously have shown that the production of $AuClPPh_3$ during ligand exchange reactions corresponds to ≈5% of the gold atoms in the nanoparticle, translating to a <2% variation in core size that falls outside the resolution of our TEM measurements. Brown, L. O. Ph.D. Dissertation, University of Oregon, Eugene, OR, 1999.

(20) This ligand exchange procedure has been employed in the exchange of 2-aminoethanethiol and (*N*,*N*,*N*-trimethylamino)ethanethiol.

(21) Alvarez, M. M.; Khoury, J. T.; Schaaff, T. G.; Shafigullin, M. N.; Vezmar, I.; Whetten, R. L. *J. Phys. Chem. B* **1997**, *101*, 3706.

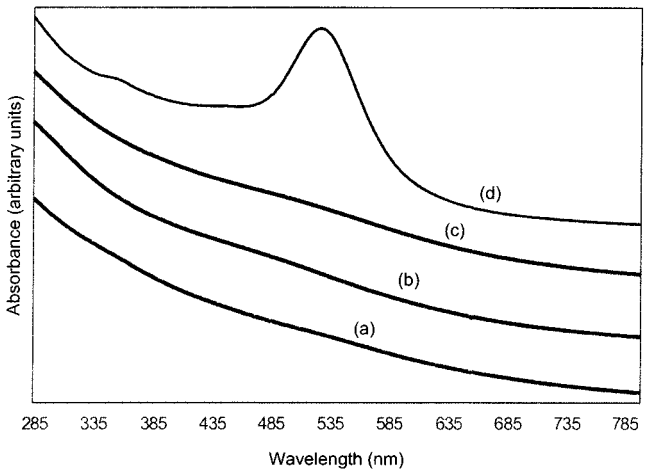

Figure 1. UV−visible spectra of (a) (*N*,*N*-dimethylamino)-ethanethiol-functionalized nanoparticle **2**, (b) partially substituted 2-mercaptoethanesulfonate nanoparticle **3**, and (c) fully functionalized 2-mercaptoethanesulfonate nanoparticle **4**. (d) Pentadecylamine-functionalized nanoparticles, having an average size of 5.0 nm, prepared via the procedure given in ref 9 have been included here as a size comparison. Note the large absorption at 528 nm corresponding to the surface plasmon resonance signifying particle with $d_{CORE} > 2$ nm.

more rapid and complete exchange prior to transfer into the aqueous phase.

Nanoparticle Characterization. Under conditions of slow ligand exchange, particle growth commonly occurs.[11] For a variety of nanoelectronic or biological applications, a small core diameter (<2 nm) and narrow dispersity are required. Therefore, measurements were performed to determine whether or not the particle size of the precursor is preserved during the exchanges. Qualitative information regarding the size of the nanoparticles is obtained from UV−visible spectroscopy, while TEM and AFM are used to obtain quantitative size measurements of representative samples (hundreds of nanoparticles of **2** and **3**). Together, these techniques demonstrate that nanoparticles **2**, **3**, and **4** retain the small gold core size and low dispersity found in the starting nanoparticle **1**.

Optical spectra of metal particles exhibit a broad absorption for interband transition and a size-dependent surface plasmon resonance band at ≈520 nm. In these samples we find the interband transition typically observed for small particles and little or no plasmon resonance consistent with a gold core size of ≈1.7 nm or less.[21] Figure 1 shows a comparison of spectra for nanoparticles **2**, **3**, and **4**.

A TEM of the cationic ligand-stabilized nanoparticle **2** (Figure 2) shows particles with no evidence of aggregation.[22] Size measurements from a collection of images such as the one shown in Figure 2 reveal particles with an average diameter of 1.4 ± 0.6 nm, in agreement with the UV−vis data reported above.

TEMs of the mixed ligand shell nanoparticle **3** revealed aggregates, which we attributed to a drying effect, based on two pieces of evidence. The addition of

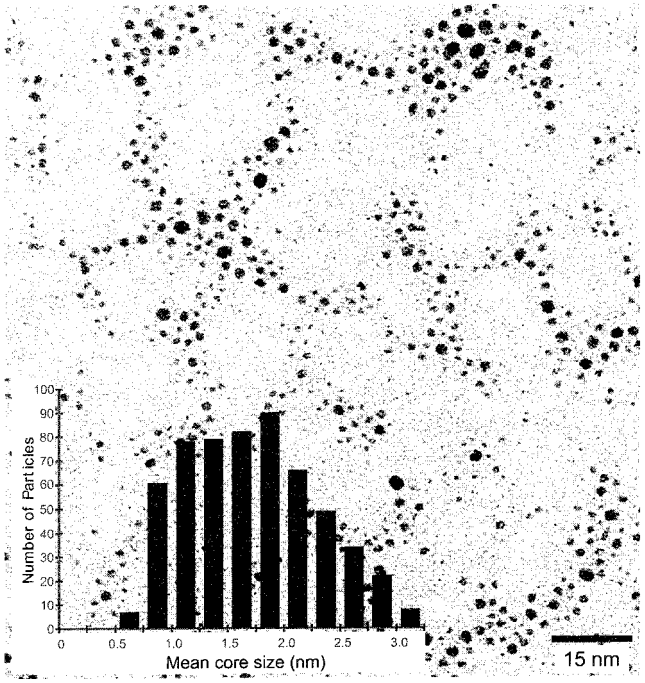

Figure 2. TEM of (*N*,*N*-dimethylamino)ethanethiol-passivated gold nanoparticle **2**. The inset shows the size distribution histogram generated from analysis of several images; 581 particles were used in the size determination and an average size of 1.4 ± 0.6 nm was determined.

methanol to the deposition solution reduced but did not eliminate the aggregates, and high concentrations of NaCl reduced the formation of aggregates. Both of these techniques resulted in frequent disruption of the TEM grid and poor quality images. AFM provided a convenient, alternative means of confirming the size of the nanoparticles. Particle heights determined by AFM for the mixed ligand shell intermediate **3** qualitatively confirm that the size and low size dispersity of the starting nanoparticles have been retained.

Nanoparticle Stability Measurements. Stability under a wide range of environmental conditions is necessary if nanoparticles are to be employed in biological or nanoelectronic applications. We examined nanoparticles **2**, **3**, and **4** for stability with elevated temperature, extremes of pH, and high salt concentrations with the goal of determining how the charge on the ω-headgroup effects nanoparticle stability. Instability of the particles could result in aggregation of the nanoparticles in solution, precipitation of intact particles due to aggregation, or decomposition of the nanoparticles that changes the metal core size.

Nanoparticle stability can be monitored by UV−vis spectroscopy because aggregation, precipitation, and decomposition each lead to distinctive changes in the spectra.[23] There were no changes in the spectra of nanoparticles **3** and **4** over 9 h at 75 °C, suggesting that both are thermally stable. Nanoparticle **2** was stable in solution at room temperature for extended periods of time, but decomposes rapidly at 75 °C.[23c] Nanoparticles **3** and **4** are stable through a broad pH range (pH = 0.2−11.5), whereas **2** decomposes rapidly under highly acidic (pH = 3) or slightly basic (pH = 8) conditions. Nanoparticles **3** and **4** were stable for weeks in solution in the presence of NaCl with no evidence of aggregation or decomposition. Nanoparticle **2** decomposes in solu-

(22) The histogram of **2** is nearly identical to that previously reported for organic-soluble alkanethiol-stabilized nanoparticles synthesized using a monophasic ligand exchange method. See ref 10 for an example of a histogram of octadecanethiol-stabilized nanoparticles produced in a monophasic ligand exchange.

tions containing high concentrations of NaCl. In each case, the 2-mercaptoethanesulfonate-stabilized nanoparticles **3** and **4** were more stable than the *N*,*N*-dimethylaminoethanethiol-stabilized particles **2**.

Solutions of **2**, **3**, and **4** each exhibited enhanced thermal stability compared to solutions of the phosphine-stabilized nanoparticles that decompose at room temperature to give bulk gold and $AuClPPh_3$.[10,24] These results are consistent with previous observations that thiol-stabilized nanoparticles exhibit greater thermal stability than phosphine-stabilized nanoparticles of the same size.[10] The instability of **2** relative to **3** and **4** likely results from reactions between the terminal dimethylamino groups and the gold surface of neighboring nanoparticles as discussed below.

The pH and salt additive studies were conducted to probe the nanoparticles' stability toward aggregation. The resistance to aggregation that was observed for all of the particles contrasts that seen for ionically stabilized colloids that typically form aggregates upon addition of salt. For example, small gold colloids ($d_{core} \approx$ 2.6 nm, prepared by thiocyanate reduction of $HAuCl_4$) and small latex spheres ($d \approx 20$ nm) containing charged surface functional groups, commonly used as biological taggants, are unstable and form aggregates in the presence of high salt concentrations.[5,25,26] Aggregation in these systems has been attributed to the reduction of the Coulombic repulsion between particles upon electrolyte addition.[27] Once the repulsive forces between the particles are reduced, van der Waals interactions bring the particles together and lead to aggregation.[27] The resistance to aggregation found in nanoparticles **2**−**4** is presumably due to the molecular layer encapsulating the nanoparticle that effectively protects the metal cores from irreversibly binding to one another, thus preventing aggregation.

We hypothesize that the relative instability of **2** to high salt concentrations and basic pH is due to the reactivity of the pendant amine toward the gold nanoparticle.[11] As electrolyte is added and the Coulombic repulsion between adjacent nanoparticles decreases, the nanoparticles approach one another, allowing the amino headgroups of adjacent particles to react at the gold surface of neighboring particles, promoting decomposition. In preliminary experiments involving a quaternized amine headgroup, no decomposition occurs, implicating the lone pair of the dimethylamino group of **2** in the decomposition pathway. Further studies of the stabilities of these and other ionically substituted nanoparticles are currently underway.

Conclusions

A simple interfacial ligand exchange approach to preparing cationic and anionic nanoparticles has been presented. The approach yields particles that are stable and water-soluble. Because the composition, size, and size dispersity of the nanoparticles depend on the mechanism and rate of ligand exchange, the interfacial exchanges reported here are more complex than those occurring in a single phase.[10] The nanoparticles produced in the interfacical exchange do retain the small core size of the parent nanoparticle; however, the reaction pathway depends on the identity of the incoming ligand. In the case where the solubility of the ligand is low in the organic phase, a partially substituted intermediate is isolated. When the charged ligand is more soluble in the organic phase, ligand exchange goes to completion in a single step. Both the anionic and cationic nanoparticles exhibit excellent stability against aggregation, although in the case of the dimethylamino headgroup, decomposition does occur under certain conditions, suggesting that the stability of the nanoparticles depends on the reactivity of the ω-headgroup. These stable, water-soluble nanoparticles are amenable to further functionalization and should prove useful for a number of applications.

Acknowledgment. We thank Dr. Robert Gilbertson for helpful discussions. This work was supported by the National Science Foundation (DMR-9705343 and CHE-9512185) and the Camille and Henry Dreyfus Foundation (J.E.H. is a Camille Dreyfus Teacher Scholar). J.E.H. is an Alfred P. Sloan Fellow.

Supporting Information Available: UV−visible spectra of **2** and ^{1}H NMR spectra of **2**, **3**, and **4**. This material is available free of charge via the Internet at http://pubs.acs.org.

CM0003875

(23) (a) Aggregation in solution results in a shift in the broad plasmon absorption.[23d] (b) Precipitation results in a uniform decrease across the absorption spectrum. (c) Decomposition of small nanoparticles usually results in either particle growth or etching. In either case, the gold-containing products exhibit new peaks in the visible spectrum. If the core size increases during the reaction, a plasmon peak at ≈520 nm grows in.[11] If the core size decreases, one observes a decrease in the interband transition and the appearance of new peaks between 300 and 500 nm analogous to those seen for Au_9 and Au_{11} species.[23e] An example UV−vis spectrum of a decomposed nanoparticle **2** sample is shown in Figure S1 in the Supporting Information. (d) Heath, J. R.; Knobler, C. M.; Leff, D. V. *J. Phys. Chem. B* **1997**, *101*, 189. (e) Bartlett, P. A.; Bauer, B.; Singer, S. J. *J. Am. Chem. Soc.* **1978**, *100*, 5085.

(24) Benfield, R. E.; Creighton, J. A.; Eadon, D. G. *Z. Phys. D. − At., Mol. Clusters* **1989**, *12*, 533.

(25) Baschong, W.; Lucocq, J. M.; Roth, J. *Histochemistry* **1985**, *83*, 409.

(26) *Working With FluoSpheres Fluorescent Microspheres*; Molecular Probes, Inc., Product Information, http://www.probes.com, 1999.

(27) *Introduction to Soft Matter*; Hamley, I. W., Ed; Wiley: Chichester, England, 2000.